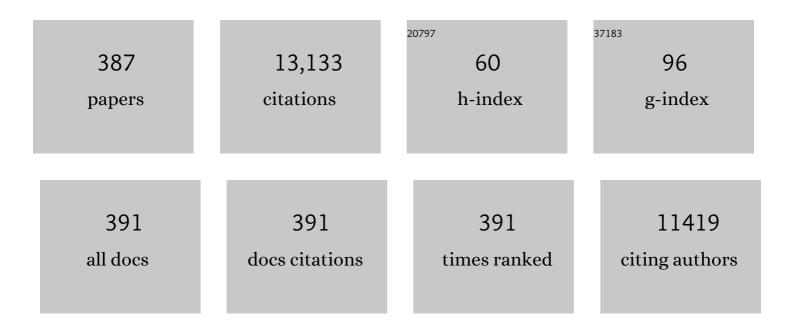
## List of Publications by Year in descending order

Source: https://exaly.com/author-pdf/4514121/publications.pdf Version: 2024-02-01



SPAMESH

#	Article	lF	CITATIONS
1	A review of polymer electrolytes: fundamental, approaches and applications. Ionics, 2016, 22, 1259-1279.	1.2	488
2	FTIR studies of PVC/PMMA blend based polymer electrolytes. Spectrochimica Acta - Part A: Molecular and Biomolecular Spectroscopy, 2007, 66, 1237-1242.	2.0	350
3	Properties of hydroxyapatite produced by annealing of bovine bone. Ceramics International, 2007, 33, 1171-1177.	2.3	345
4	Porous hydroxyapatite for artificial bone applications. Science and Technology of Advanced Materials, 2007, 8, 116-123.	2.8	342
5	The effects of sintering temperature on the properties of hydroxyapatite. Ceramics International, 2000, 26, 221-230.	2.3	334
6	Fundamental Concepts of Hydrogels: Synthesis, Properties, and Their Applications. Polymers, 2020, 12, 2702.	2.0	321
7	Design of thin wall structures for energy absorption applications: Enhancement of crashworthiness due to axial and oblique impact forces. Thin-Walled Structures, 2013, 71, 7-17.	2.7	223
8	A review on microstructural study and compressive strength of geopolymer mortar, paste and concrete. Construction and Building Materials, 2018, 186, 550-576.	3.2	202
9	Conductivity and FTIR studies on PEO–LiX [X: CF3SO3â^', SO42â^'] polymer electrolytes. Spectrochimica Acta - Part A: Molecular and Biomolecular Spectroscopy, 2008, 69, 670-675.	2.0	171
10	Facile sonochemical synthesis of nanostructured NiO with different particle sizes and its electrochemical properties for supercapacitor application. Journal of Colloid and Interface Science, 2016, 471, 136-144.	5.0	171
11	Good prospect of ionic liquid based-poly(vinyl alcohol) polymer electrolytes for supercapacitors with excellent electrical, electrochemical and thermal properties. International Journal of Hydrogen Energy, 2014, 39, 2953-2963.	3.8	167
12	Ultrahigh capacitance of amorphous nickel phosphate for asymmetric supercapacitor applications. RSC Advances, 2016, 6, 76298-76306.	1.7	167
13	Preparation and characterization of nanocellulose reinforced semi-interpenetrating polymer network of chitosan hydrogel. Cellulose, 2017, 24, 2215-2228.	2.4	148
14	Synthesis and sintering of hydroxyapatite derived from eggshells as a calcium precursor. Ceramics International, 2014, 40, 16349-16359.	2.3	145
15	Ion conducting corn starch biopolymer electrolytes doped with ionic liquid 1-butyl-3-methylimidazolium hexafluorophosphate. Journal of Non-Crystalline Solids, 2011, 357, 3654-3660.	1.5	144
16	A review on resistance spot welding of aluminum alloys. International Journal of Advanced Manufacturing Technology, 2017, 90, 605-634.	1.5	137
17	Effect of ethylene carbonate on the ionic conduction in poly(vinylidenefluoride-hexafluoropropylene) based solid polymer electrolytes. Polymer Chemistry, 2010, 1, 702.	1.9	135
18	Enhanced electrochemical performance of cobalt oxide nanocube intercalated reduced graphene oxide for supercapacitor application. RSC Advances, 2016, 6, 34894-34902.	1.7	131

#	Article	IF	CITATIONS
19	Structural, thermal and electrochemical cell characteristics of poly(vinyl chloride)-based polymer electrolytes. Journal of Power Sources, 2001, 99, 41-47.	4.0	124
20	Characterization of ionic liquid added poly(vinylÂalcohol)-based proton conducting polymer electrolytes and electrochemical studiesÂon the supercapacitors. International Journal of Hydrogen Energy, 2015, 40, 852-862.	3.8	114
21	Electrical, structural, thermal and electrochemical properties of corn starch-based biopolymer electrolytes. Carbohydrate Polymers, 2015, 124, 222-228.	5.1	112
22	Densification behaviour of nanocrystalline hydroxyapatite bioceramics. Journal of Materials Processing Technology, 2008, 206, 221-230.	3.1	107
23	Challenges and advances in laser welding of dissimilar light alloys: Al/Mg, Al/Ti, and Mg/Ti alloys. International Journal of Advanced Manufacturing Technology, 2018, 95, 4353-4369.	1.5	107
24	A review on laser beam welding of titanium alloys. International Journal of Advanced Manufacturing Technology, 2018, 97, 1071-1098.	1.5	101
25	Characterization of biogenic hydroxyapatite derived from animal bones for biomedical applications. Ceramics International, 2018, 44, 10525-10530.	2.3	95
26	Curcumin/Tween 20-incorporated cellulose nanoparticles with enhanced curcumin solubility for nano-drug delivery: characterization and in vitro evaluation. Cellulose, 2019, 26, 5467-5481.	2.4	93
27	Processing of mesoporous silica materials (MCM-41) from coal fly ash. Journal of Materials Processing Technology, 2007, 186, 8-13.	3.1	92
28	Influence of a nonionic surfactant on curcumin delivery of nanocellulose reinforced chitosan hydrogel. International Journal of Biological Macromolecules, 2018, 118, 1055-1064.	3.6	90
29	Conducting polymer and its composite materials based electrochemical sensor for Nicotinamide Adenine Dinucleotide (NADH). Biosensors and Bioelectronics, 2016, 79, 763-775.	5.3	88
30	Electrocoagulation treatment of raw landfill leachate using iron-based electrodes: Effects of process parameters and optimization. Journal of Environmental Management, 2017, 204, 75-81.	3.8	88
31	Investigation on the effects of addition of SiO2 nanoparticles on ionic conductivity, FTIR, and thermal properties of nanocomposite PMMA–LiCF3SO3–SiO2. Ionics, 2010, 16, 255-262.	1.2	87
32	Sintering behaviour of natural porous hydroxyapatite derived from bovine bone. Ceramics International, 2015, 41, 3024-3029.	2.3	87
33	Electrical, structural, and thermal studies of antimony trioxide-doped poly(acrylic acid)-based composite polymer electrolytes. Ionics, 2014, 20, 665-674.	1.2	86
34	Consolidation of nanocrystalline hydroxyapatite powder. Science and Technology of Advanced Materials, 2007, 8, 124-130.	2.8	85
35	Advanced composite sandwich structure design for energy absorption applications: Blast protection and crashworthiness. Composites Part B: Engineering, 2012, 43, 2198-2208.	5.9	85
36	Sintering properties of hydroxyapatite powders prepared using different methods. Ceramics International, 2013, 39, 111-119.	2.3	85

#	Article	IF	CITATIONS
37	Investigation on structural and electrochemical properties of binder free nanostructured nickel oxide thin film. Materials Letters, 2015, 161, 694-697.	1.3	82
38	Direct conversion of eggshell to hydroxyapatite ceramic by a sintering method. Ceramics International, 2016, 42, 7824-7829.	2.3	82
39	Fuzzy logic based model for predicting surface roughness of machined Al–Si–Cu–Fe die casting alloy using different additives-turning. Measurement: Journal of the International Measurement Confederation, 2015, 61, 150-161.	2.5	80
40	An enhanced performance of hybrid supercapacitor based on polyaniline-manganese phosphate binary composite. Journal of Solid State Electrochemistry, 2017, 21, 3205-3213.	1.2	79
41	Comparison between microwave and conventional sintering on the properties and microstructural evolution of tetragonal zirconia. Ceramics International, 2018, 44, 8922-8927.	2.3	79
42	Rapid densification of nanocrystalline hydroxyapatite for biomedical applications. Ceramics International, 2007, 33, 1363-1367.	2.3	78
43	Characterization of conducting cellulose acetate based polymer electrolytes doped with "green― ionic mixture. Carbohydrate Polymers, 2013, 91, 14-21.	5.1	78
44	Synthesis, characterization, properties of N-succinyl chitosan-g-poly (methacrylic acid) hydrogels and inÂvitro release of theophylline. Polymer, 2016, 92, 36-49.	1.8	77
45	Microstructure and mechanical properties of resistance spot welded in welding-brazing mode and resistance element welded magnesium alloy/austenitic stainless steel joints. Journal of Materials Processing Technology, 2017, 250, 45-54.	3.1	76
46	Sintering, microstructure and mechanical properties of commercial Y-TZPs. Journal of Materials Science, 1996, 31, 6055-6062.	1.7	74
47	Preparation and characterization of lithium ion conducting ionic liquid-based biodegradable corn starch polymer electrolytes. Journal of Solid State Electrochemistry, 2012, 16, 1869-1875.	1.2	74
48	Enhanced ionic conductivity of scandia-ceria-stabilized-zirconia (10Sc1CeSZ) electrolyte synthesized by the microwave-assisted glycine nitrate process. Ceramics International, 2017, 43, 8119-8125.	2.3	73
49	Electric double-layer capacitors with corn starch-based biopolymer electrolytes incorporating silica as filler. Ionics, 2015, 21, 2061-2068.	1.2	72
50	An Approach to Solid-State Electrical Double Layer Capacitors Fabricated with Graphene Oxide-Doped, Ionic Liquid-Based Solid Copolymer Electrolytes. Materials, 2016, 9, 450.	1.3	70
51	Ionic liquid enhanced magnesium-based polymer electrolytes for electrical double-layer capacitors. Ionics, 2016, 22, 919-925.	1.2	70
52	Hydroxypropyl Cellulose Based Non-Volatile Gel Polymer Electrolytes for Dye-Sensitized Solar Cell Applications using 1-methyl-3-propylimidazolium iodide ionic liquid. Scientific Reports, 2015, 5, 18056.	1.6	68
53	Investigating the Machinability of Al–Si–Cu cast alloy containing bismuth and antimony using coated carbide insert. Measurement: Journal of the International Measurement Confederation, 2015, 62, 170-178.	2.5	68
54	Effects of silicate and carbonate substitution on the properties of hydroxyapatite prepared by aqueous co-precipitation method. Materials and Design, 2015, 87, 788-796.	3.3	67

#	Article	IF	CITATIONS
55	pH responsive N-succinyl chitosan/Poly (acrylamide-co-acrylic acid) hydrogels and in vitro release of 5-fluorouracil. PLoS ONE, 2017, 12, e0179250.	1.1	67
56	A review on laser beam welding of copper alloys. International Journal of Advanced Manufacturing Technology, 2018, 96, 475-490.	1.5	67
57	Preparation and Characterization of Poly(lactic Acid)-based Composite Reinforced with Oil Palm Empty Fruit Bunch Fiber and Nanosilica. BioResources, 2015, 11, .	0.5	66
58	Characteristics and properties of hydoxyapatite derived by sol–gel and wet chemical precipitation methods. Ceramics International, 2015, 41, 10434-10441.	2.3	66
59	Studies on the plasticization efficiency of deep eutectic solvent in suppressing the crystallinity of corn starch based polymer electrolytes. Carbohydrate Polymers, 2012, 87, 701-706.	5.1	65
60	Microwave pyrolysis of oil palm fiber (OPF) for hydrogen production: Parametric investigation. Energy Conversion and Management, 2016, 115, 232-243.	4.4	65
61	Composite sandwich structures with nested inserts for energy absorption application. Composite Structures, 2012, 94, 904-916.	3.1	63
62	Comparing Triflate and Hexafluorophosphate Anions of Ionic Liquids in Polymer Electrolytes for Supercapacitor Applications. Materials, 2014, 7, 4019-4033.	1.3	63
63	Electric double layer capacitor based on activated carbon electrode and biodegradable composite polymer electrolyte. Ionics, 2014, 20, 251-258.	1.2	63
64	A review on the hydrothermal ageing behaviour of Y-TZP ceramics. Ceramics International, 2018, 44, 20620-20634.	2.3	63
65	Nanocrystalline forsterite for biomedical applications: Synthesis, microstructure and mechanical properties. Journal of the Mechanical Behavior of Biomedical Materials, 2013, 25, 63-69.	1.5	62
66	A review on resistance spot welding of magnesium alloys. International Journal of Advanced Manufacturing Technology, 2016, 86, 1805-1825.	1.5	62
67	Densification behaviour and properties of manganese oxide doped Y-TZP ceramics. Ceramics International, 2011, 37, 3583-3590.	2.3	61
68	Impact of low viscosity ionic liquid on PMMA–PVC–LiTFSI polymer electrolytes based on AC -impedance, dielectric behavior, and HATR–FTIR characteristics. Journal of Materials Research, 2012, 27, 2996-3004.	1.2	61
69	Oxide scale growth and presumed exfoliation in a 700°C or higher steam condition: A simulation study for future operations of ultra-supercritical power plants. Journal of Supercritical Fluids, 2014, 92, 215-222.	1.6	61
70	The effect of manganese oxide on the sinterability of hydroxyapatite. Science and Technology of Advanced Materials, 2007, 8, 257-263.	2.8	60
71	Effect of manganese oxide on the sintered properties and low temperature degradation of Y-TZP ceramics. Ceramics International, 2008, 34, 1603-1608.	2.3	60
72	Effects of manganese doping on properties of sol–gel derived biphasic calcium phosphate ceramics. Ceramics International, 2011, 37, 3703-3715.	2.3	60

#	Article	IF	CITATIONS
73	Sintering behavior of hydroxyapatite prepared from different routes. Materials & Design, 2012, 34, 148-154.	5.1	60
74	Sintering and mechanical properties of MgO-doped nanocrystalline hydroxyapatite. Ceramics International, 2013, 39, 8979-8983.	2.3	60
75	The Effects of Calciumâ€ŧoâ€Phosphorus Ratio on the Densification and Mechanical Properties of Hydroxyapatite Ceramic. International Journal of Applied Ceramic Technology, 2015, 12, 223-227.	1.1	60
76	Effect of two-step sintering on the hydrothermal ageing resistance of tetragonal zirconia polycrystals. Ceramics International, 2017, 43, 7594-7599.	2.3	59
77	Nonsurfactant route of fatty alcohols decomposition for templating of mesoporous silica. Microporous and Mesoporous Materials, 2008, 112, 243-253.	2.2	58
78	Effects of bismuth oxide on the sinterability of hydroxyapatite. Ceramics International, 2011, 37, 599-606.	2.3	58
79	Poly(Acrylic acid)–Based Hybrid Inorganic–Organic Electrolytes Membrane for Electrical Double Layer Capacitors Application. Polymers, 2016, 8, 179.	2.0	58
80	Non-hydrothermal synthesis of mesoporous materials using sodium silicate from coal fly ash. Materials Chemistry and Physics, 2007, 101, 344-351.	2.0	57
81	Effect of multi-ions doping on the properties of carbonated hydroxyapatite bioceramic. Ceramics International, 2019, 45, 3473-3477.	2.3	57
82	Novel poly(vinylidene fluoride-co-hexafluoro propylene)/polyethylene oxide based gel polymer electrolyte containing fumed silica (SiO2) nanofiller for high performance dye-sensitized solar cell. Electrochimica Acta, 2016, 220, 573-580.	2.6	56
83	Environmental degradation of CuO-doped Y-TZP ceramics. Ceramics International, 2001, 27, 705-711.	2.3	55
84	Augmented reality–based programming, planning and simulation of a robotic work cell. Proceedings of the Institution of Mechanical Engineers, Part B: Journal of Engineering Manufacture, 2015, 229, 1029-1045.	1.5	55
85	A facile ultrasonic-aided biosynthesis of ZnO nanoparticles using Vaccinium arctostaphylos L. leaf extract and its antidiabetic, antibacterial, and oxidative activity evaluation. Ultrasonics Sonochemistry, 2019, 55, 57-66.	3.8	55
86	A concise review on corrosion inhibitors: types, mechanisms and electrochemical evaluation studies. Journal of Coatings Technology Research, 2022, 19, 241-268.	1.2	55
87	Title is missing!. Journal of Materials Science, 1999, 34, 5457-5467.	1.7	54
88	Sonochemical synthesis of nanostructured nickel hydroxide as an electrode material for improved electrochemical energy storage application. Progress in Natural Science: Materials International, 2017, 27, 416-423.	1.8	54
89	Impedance spectroscopy of CuO-doped Y-TZP ceramics. Journal of Materials Science, 1998, 33, 5103-5110.	1.7	53
90	Conductivity, dielectric behaviour and thermal stability studies of lithium ion dissociation in poly(methyl methacrylate)-based gel polymer electrolytes. Ionics, 2009, 15, 249-254.	1.2	53

#	Article	IF	CITATIONS
91	The role and contribution of green buildings on sustainable development goals. Building and Environment, 2020, 185, 107091.	3.0	53
92	Machining characteristics of Inconel 718 under several cutting conditions based on Taguchi method. Proceedings of the Institution of Mechanical Engineers, Part C: Journal of Mechanical Engineering Science, 2013, 227, 1889-1897.	1.1	52
93	Electrophoretic deposition of magnesium silicates on titanium implants: Ion migration and silicide interfaces. Applied Surface Science, 2014, 307, 1-6.	3.1	52
94	N-succinyl chitosan preparation, characterization, properties and biomedical applications: a state of the art review. Reviews in Chemical Engineering, 2015, 31, .	2.3	51
95	Effect of different imidazolium-based ionic liquids on gel polymer electrolytes for dye-sensitized solar cells. Ionics, 2019, 25, 2427-2435.	1.2	51
96	Impedance and FTIR studies on plasticized PMMA–LiN(CF3SO2)2 nanocomposite polymer electrolytes. Ionics, 2010, 16, 465-473.	1.2	49
97	A novel design, analysis and 3D printing of Ti-6Al-4V alloy bio-inspired porous femoral stem. Journal of Materials Science: Materials in Medicine, 2020, 31, 78.	1.7	48
98	Ternary nanocomposite of cobalt oxide nanograins and silver nanoparticles grown on reduced graphene oxide conducting platform for high-performance supercapattery electrode material. Journal of Alloys and Compounds, 2020, 821, 153452.	2.8	46
99	Efficiency improvement by incorporating 1-methyl-3-propylimidazolium iodide ionic liquid in gel polymer electrolytes for dye-sensitized solar cells. Electrochimica Acta, 2015, 175, 169-175.	2.6	45
100	Studies on ionic liquid-based corn starch biopolymer electrolytes coupling with high ionic transport number. Cellulose, 2013, 20, 3227-3237.	2.4	44
101	The conductivity and dielectric studies of solid polymer electrolytes based on poly (acrylamide-co-acrylic acid) doped with sodium iodide. Ionics, 2018, 24, 1947-1953.	1.2	44
102	The properties of hydroxyapatite ceramic coatings produced by plasma electrolytic oxidation. Ceramics International, 2018, 44, 1802-1811.	2.3	44
103	Evolution of sustainability in global green building rating tools. Journal of Cleaner Production, 2020, 259, 120912.	4.6	44
104	Formulation and characterization of hybrid polymeric/ZnO nanocomposite coatings with remarkable anti-corrosion and hydrophobic characteristics. Journal of Coatings Technology Research, 2016, 13, 921-930.	1.2	43
105	Degradation of ultra-high molecular weight poly(methyl methacrylate-co-butyl acrylate-co-acrylic) Tj ETQq1 1	0.784314 rg 1.7	BT /Qverlock
106	Rheological behavior of biodegradable N-succinyl chitosan-g-poly (acrylic acid) hydrogels and their applications as drug carrier and in vitro theophylline release. International Journal of Biological Macromolecules, 2018, 117, 454-466.	3.6	43
107	Development of asymmetric device using Co3(PO4)2 as a positive electrode for energy storage application. Journal of Materials Science: Materials in Electronics, 2019, 30, 7435-7446.	1.1	43
108	Binary nanocomposite based on Co3O4 nanocubes and multiwalled carbon nanotubes as an ultrasensitive platform for amperometric determination of dopamine. Mikrochimica Acta, 2017, 184, 2739-2748.	2.5	42

#	Article	IF	CITATIONS
109	Investigation on the effect of nanosilica towards corn starch–lithium perchlorate-based polymer electrolytes. Journal of Solid State Electrochemistry, 2012, 16, 3165-3170.	1.2	40
110	The influence of Ca/P ratio on the properties of hydroxyapatite bioceramics. Proceedings of SPIE, 2007, 6423, 855.	0.8	39
111	Micro-arc oxidation of bioceramic coatings containing eggshell-derived hydroxyapatite on titanium substrate. Ceramics International, 2019, 45, 18371-18381.	2.3	39
112	Sintering behaviour and properties of manganese-doped alumina. Ceramics International, 2019, 45, 7049-7054.	2.3	39
113	Finite element study of functionally graded porous femoral stems incorporating bodyâ€centered cubic structure. Artificial Organs, 2019, 43, E152-E164.	1.0	38
114	Rheological Studies of PMMA–PVC Based Polymer Blend Electrolytes with LiTFSI as Doping Salt. PLoS ONE, 2014, 9, e102815.	1.1	37
115	Effect of different iodide salts on ionic conductivity and structural and thermal behavior of rice-starch-based polymer electrolytes for dye-sensitized solar cell application. Ionics, 2015, 21, 2383-2391.	1.2	35
116	Effects of ionic liquid on the hydroxylpropylmethyl cellulose (HPMC) solid polymer electrolyte. Ionics, 2016, 22, 2421-2430.	1.2	34
117	Analysis of corrosion protection behavior of Al2O3-TiO2 oxide ceramic coating on carbon steel pipes for petroleum industry. Ceramics International, 2018, 44, 5967-5975.	2.3	34
118	Effect of zinc ions on the structural characteristics of hydroxyapatite bioceramics. Ceramics International, 2020, 46, 13945-13952.	2.3	34
119	Sintering behaviour and properties of graphene oxide-doped Y-TZP ceramics. Ceramics International, 2016, 42, 17620-17625.	2.3	33
120	Conductivity, dielectric studies and structural properties of P(VA-co-PE) and its application in dye sensitized solar cell. Organic Electronics, 2018, 56, 116-124.	1.4	33
121	Effect of pH on the properties of eggshell-derived hydroxyapatite bioceramic synthesized by wet chemical method assisted by microwave irradiation. Ceramics International, 2021, 47, 8879-8887.	2.3	33
122	FTIR spectra of plasticized high molecular weight PVC–LiCF3SO3 electrolytes. Ionics, 2009, 15, 413-420.	1.2	31
123	Comparison of the performance of copper oxide and yttrium oxide nanoparticle based hydroxylethyl cellulose electrolytes for supercapacitors. Journal of Applied Polymer Science, 2017, 134, .	1.3	31
124	The conductivity and dielectric studies of polymer electrolytes based on iota-carrageenan with sodium iodide and 1-butyl-3-methylimidazolium iodide for the dye-sensitized solar cells. Ionics, 2019, 25, 763-771.	1.2	31
125	Poly (1-vinylpyrrolidone-co-vinyl acetate) (PVP-co-VAc) based gel polymer electrolytes for electric double layer capacitors (EDLC). Journal of Polymer Research, 2020, 27, 1.	1.2	31
126	Electrical, thermal, and structural studies on highly conducting additive-free biopolymer electrolytes for electric double-layer capacitor application. Ionics, 2019, 25, 4861-4874.	1.2	30

#	Article	IF	CITATIONS
127	Effect of dibutyl phthalate as plasticizer on high-molecular weight poly(vinyl chloride)–lithium tetraborate-based solid polymer electrolytes. Ionics, 2011, 17, 705-713.	1.2	29
128	Effect of Ag nanoparticles seeding on the properties of silica spheres. Ceramics International, 2018, 44, 5901-5908.	2.3	28
129	Preparation and characterization of poly (ethyl methacrylate) based polymer electrolytes doped with 1-butyl-3-methylimidazolium trifluoromethanesulfonate. Measurement: Journal of the International Measurement Confederation, 2014, 48, 263-273.	2.5	27
130	Conductivity, Mechanical and Thermal Studies on Poly(methyl methacrylate)-Based Polymer Electrolytes Complexed with Lithium Tetraborate and Propylene Carbonate. Journal of Materials Engineering and Performance, 2012, 21, 89-94.	1.2	26
131	Studies on biodegradable polymer electrolyte rice starch (RS) complexed with lithium iodide. Ionics, 2014, 20, 691-695.	1.2	26
132	Sintering behaviour of carbonated hydroxyapatite prepared at different carbonate and phosphate ratios. Boletin De La Sociedad Espanola De Ceramica Y Vidrio, 2020, 59, 73-80.	0.9	26
133	Effects of sintering additives on the densification and properties of alumina-toughened zirconia ceramic composites. Ceramics International, 2020, 46, 27539-27549.	2.3	26
134	Preparation and characterization of starch-based bioplastic composites with treated oil palm empty fruit bunch fibers and citric acid. Cellulose, 2021, 28, 4191-4210.	2.4	26
135	Exploring the effect of novel N-butyl-6-methylquinolinium bis(trifluoromethylsulfonyl)imide ionic liquid addition to poly(methyl methacrylate-co-methacrylic) acid electrolyte system as employed in gel-state dye sensitized solar cells. Electrochimica Acta, 2017, 240, 361-370.	2.6	25
136	Electrical, dielectric and electrochemical characterization of novel poly(acrylic acid)-based polymer electrolytes complexed with lithium tetrafluoroborate. Chemical Physics Letters, 2018, 692, 19-27.	1.2	25
137	A systematic review on material selection methods. Proceedings of the Institution of Mechanical Engineers, Part L: Journal of Materials: Design and Applications, 2020, 234, 1032-1059.	0.7	25
138	Preparation and characterization of plasticized high molecular weight PVC-based polymer electrolytes. Sadhana - Academy Proceedings in Engineering Sciences, 2010, 35, 87-95.	0.8	24
139	Enhancement of ionic conductivity and structural properties by 1â€butylâ€3â€methylimidazolium trifluoromethanesulfonate ionic liquid in poly(vinylidene fluoride–hexafluoropropylene)â€based polymer electrolytes. Journal of Applied Polymer Science, 2012, 126, E484.	1.3	24
140	Discussion on the influence of DES content in CA-based polymer electrolytes. Journal of Materials Science, 2012, 47, 1787-1793.	1.7	24
141	Density functional theory simulation of cobalt oxide aggregation and facile synthesis of a cobalt oxide, gold and multiwalled carbon nanotube based ternary composite for a high performance supercapattery. New Journal of Chemistry, 2019, 43, 13183-13195.	1.4	24
142	Characterization of soft-combustion-derived NASICON-type Li2Co2(MoO4)3 for lithium batteries. Materials Chemistry and Physics, 2004, 87, 318-326.	2.0	23
143	Preparation and performance analysis of barium titanate incorporated in corn starchâ€based polymer electrolytes for electric double layer capacitor application. Journal of Applied Polymer Science, 2016, 133, .	1.3	23
144	The potential of incorporation of binary salts and ionic liquid in P(VP-co-VAc) gel polymer electrolyte in electrochemical and photovoltaic performances. Scientific Reports, 2016, 6, 27630.	1.6	22

#	Article	IF	CITATIONS
145	Microwave sintering of ceria-doped scandia stabilized zirconia as electrolyte for solid oxide fuel cell. International Journal of Hydrogen Energy, 2016, 41, 14184-14190.	3.8	22
146	Novel development towards preparation of highly efficient ionic liquid based co-polymer electrolytes and its application in dye-sensitized solar cells. Organic Electronics, 2017, 41, 33-41.	1.4	22
147	Cobalt Oxide Nanograins and Silver Nanoparticles Decorated Fibrous Polyaniline Nanocomposite as Battery-Type Electrode for High Performance Supercapattery. Polymers, 2020, 12, 2816.	2.0	22
148	Na-doped LiMnPO4 as an electrode material for enhanced lithium ion batteries. Bulletin of Materials Science, 2017, 40, 171-175.	0.8	21
149	Quasi-solid-state agar-based polymer electrolytes for dye-sensitized solar cell applications using imidazolium-based ionic liquid. Ionics, 2017, 23, 1585-1590.	1.2	21
150	Resistance element weld-bonding and resistance spot weld-bonding of Mg alloy/austenitic stainless steel. Journal of Manufacturing Processes, 2019, 48, 12-30.	2.8	21
151	Effect of sintering temperature on the morphology, crystallinity and mechanical properties of carbonated hydroxyapatite (CHA). Ceramics International, 2020, 46, 26784-26789.	2.3	21
152	Mechanical studies on poly(vinyl chloride)–poly(methyl methacrylate)-based polymer electrolytes. Journal of Materials Science, 2010, 45, 1280-1283.	1.7	20
153	Ionic conductivity, dielectric behavior, and HATR–FTIR analysis onto poly(methyl) Tj ETQq1 1 0.784314 rgBT /v Polymer Science, 2013, 127, 2380-2388.	Overlock 1 1.3	0 Tf 50 427 20
154	Optimization of poly(vinyl alcohol-co-ethylene)-based gel polymer electrolyte containing nickel phosphate nanoparticles for dye-sensitized solar cell application. Solar Energy, 2019, 178, 231-240.	2.9	20
155	A study incorporating nano-sized silica into PVC-blend-based polymer electrolytes for lithium batteries. Journal of Materials Science, 2009, 44, 6404-6407.	1.7	19
156	Structural, thermal, and conductivity studies of high molecular weight poly(vinylchloride)-lithium triflate polymer electrolyte plasticized by dibutyl phthalate. Ionics, 2009, 15, 725-730.	1.2	19
157	Development and investigation on PMMA–PVC blend-based solid polymer electrolytes with LiTFSI as dopant salt. Polymer Bulletin, 2013, 70, 1277-1288.	1.7	19
158	Exact solution for stresses/displacements in a multilayered hollow cylinder under thermo-mechanical loading. International Journal of Pressure Vessels and Piping, 2017, 151, 45-53.	1.2	19
159	Exploration on polypropylene carbonate polymer for gel polymer electrolyte preparation and dyeâ€sensitized solar cell application. Journal of Applied Polymer Science, 2017, 134, 45091.	1.3	19
160	Two-Step Sintering of Ceramics. , 0, , .		19
161	Resistance element welding of magnesium alloy and austenitic stainless steel in three-sheet configurations. Journal of Materials Processing Technology, 2019, 274, 116292.	3.1	19
162	Polyacrylonitrile–poly(1â€vinyl pyrrolidoneâ€ <i>co</i> â€vinyl acetate) blend based gel polymer electrolytes incorporated with sodium iodide salt for dyeâ€sensitized solar cell applications. Journal of Applied Polymer Science, 2019, 136, 47810.	1.3	19

#	Article	IF	CITATIONS
163	Synthesis and characterization of silica nanospheres using nonsurfactant template. Ceramics International, 2013, 39, 931-940.	2.3	18
164	Development of a bone substitute material based on alpha-tricalcium phosphate scaffold coated with carbonate apatite/poly-epsilon-caprolactone. Biomedical Materials (Bristol), 2015, 10, 045011.	1.7	18
165	Passively Q-switched erbium-doped fibre laser using cobalt oxide nanocubes as a saturable absorber. Journal of Modern Optics, 2017, 64, 1315-1320.	0.6	18
166	Is Graphitic Silicon Carbide (Silagraphene) Stable?. Chemistry of Materials, 2018, 30, 7234-7244.	3.2	18
167	Sintering behavior of anorthite-based composite ceramics produced from natural phosphate and kaolin. Ceramics International, 2019, 45, 20258-20265.	2.3	18
168	Synthesis and redox properties of LixNi2(MoO4)3: a new 3-V class positive electrode material for rechargeable lithium batteries. Journal of Electroanalytical Chemistry, 2004, 570, 107-112.	1.9	17
169	Sintering and Properties of Dense Manganese-Doped Calcium Phosphate Bioceramics Prepared Using Sol-Gel Derived Nanopowders. Materials and Manufacturing Processes, 2011, 26, 908-914.	2.7	17
170	Employment of [Amim] Cl in the effort to upgrade the properties of cellulose acetate based polymer electrolytes. Cellulose, 2013, 20, 1377-1389.	2.4	17
171	Studies on the Influence of Titania Content on the Properties of Poly(vinyl chloride) - Poly (acrylonitrile)-Based Polymer Electrolytes. Polymer-Plastics Technology and Engineering, 2013, 52, 1474-1481.	1.9	17
172	Influence of pH on the physical and electromagnetic properties of Mg–Mn ferrite synthesized by a solution combustion method. Materials Characterization, 2015, 110, 109-115.	1.9	17
173	Effects of sintering on the mechanical and ionic properties of ceria-doped scandia stabilized zirconia ceramic. Ceramics International, 2016, 42, 14469-14474.	2.3	17
174	Quasi solid-state dye-sensitized solar cell with P(MMA-co-MAA)-based polymer electrolytes. Journal of Solid State Electrochemistry, 2019, 23, 1179-1189.	1.2	17
175	Influence of electrodeposited Cu-Ni layer on interfacial reaction and mechanical properties of laser welded-brazed Mg/Ti lap joints. Journal of Manufacturing Processes, 2019, 37, 251-265.	2.8	17
176	Effect of microwave sintering on the properties of copper oxide doped Y-TZP ceramics. Ceramics International, 2018, 44, 19639-19645.	2.3	16
177	Coral-like structured nickel sulfide-cobalt sulfide binder-free electrode for supercapattery. Ionics, 2020, 26, 3621-3630.	1.2	16
178	A fuzzy model for evaluation and prediction of slurry erosion of 5127 steels. Materials & Design, 2012, 39, 186-191.	5.1	15
179	Sintering behaviour and properties of magnesium orthosilicate-hydroxyapatite ceramic. Ceramics International, 2016, 42, 15756-15761.	2.3	15
180	Wettability, structural and optical properties investigation of TiO2 nanotubular arrays. Materials Research Bulletin, 2016, 78, 179-185.	2.7	15

#	Article	IF	CITATIONS
181	Poly(vinyl alcohol)-α-chitin composites reinforced by oil palm empty fruit bunch fiber-derived nanocellulose. International Journal of Polymer Analysis and Characterization, 2017, 22, 294-304.	0.9	15
182	Influence of sodium on the properties of sol-gel derived hydroxyapatite powder and porous scaffolds. Ceramics International, 2017, 43, 12263-12269.	2.3	15
183	Ionic conductivity improvement in poly (propylene) carbonate-based gel polymer electrolytes using 1-butyl-3-methylimidazolium iodide (BmimI) ionic liquid for dye-sensitized solar cell application. Ionics, 2017, 23, 1601-1605.	1.2	15
184	Comparative study on the corrosion and wear behavior of plasma-sprayed vs. high velocity oxygen fuel-sprayed Al8Si20BN ceramic coatings. Ceramics International, 2018, 44, 12180-12193.	2.3	15
185	Investigation on gel polymer electrolyte-based dye-sensitized solar cells using carbon nanotube. Ionics, 2019, 25, 319-325.	1.2	15
186	lota-carrageenan-based polymer electrolyte: impact on ionic conductivity with incorporation of AmNTFSI ionic liquid for supercapacitor. Ionics, 2019, 25, 3321-3329.	1.2	15
187	Effect of copper-nickel interlayer thickness on laser welding-brazing of Mg/Ti alloy. Optics and Laser Technology, 2019, 115, 149-159.	2.2	15
188	Poly(lactic acid) composite films reinforced with microcrystalline cellulose and keratin from chicken feather fiber in 1â€butylâ€3â€methylimidazolium chloride. Journal of Applied Polymer Science, 2019, 136, 47642.	1.3	15
189	Mechanochemical Synthesis of Nanosized Hydroxyapatite Powder and its Conversion to Dense Bodies. Materials Science Forum, 0, 694, 118-122.	0.3	14
190	High operating steam pressure and localized overheating of a primary superheater tube. Engineering Failure Analysis, 2012, 26, 344-348.	1.8	14
191	Simulating the implications of oxide scale formations in austenitic steels of ultra-supercritical fossil power plants. Engineering Failure Analysis, 2014, 42, 390-401.	1.8	14
192	A new thio-Schiff base fluorophore with copper ion sensing, DNA binding and nuclease activity. Spectrochimica Acta - Part A: Molecular and Biomolecular Spectroscopy, 2015, 150, 175-180.	2.0	14
193	Fabrication and Compressive Properties of Low to Medium Porosity Closed-Cell Porous Aluminum Using PMMA Space Holder Technique. Materials, 2016, 9, 254.	1.3	14
194	Virtual Planning, Control, and Machining for a Modular-Based Automated Factory Operation in an Augmented Reality Environment. Scientific Reports, 2016, 6, 27380.	1.6	14
195	Corrosion protection performance of nanocomposite coatings under static, UV, and dynamic conditions. Journal of Coatings Technology Research, 2018, 15, 1035-1047.	1.2	14
196	Novel palladium-guanine-reduced graphene oxide nanocomposite as efficient electrocatalyst for methanol oxidation reaction. Materials Research Bulletin, 2019, 112, 213-220.	2.7	14
197	HEAT TRANSFER MODEL FOR PREDICTING SURVIVAL TIME IN COLD WATER IMMERSION. Biomedical Engineering - Applications, Basis and Communications, 2005, 17, 159-166.	0.3	13
198	Effect of Short Time Sintering on the Mechanical Properties of Undoped Zirconia Ceramics. Applied Mechanics and Materials, 0, 629, 420-425.	0.2	13

#	Article	IF	CITATIONS
199	Stress intensity factors of a corner crack emanating from a pinhole of a solid cylinder. Engineering Fracture Mechanics, 2014, 128, 1-7.	2.0	13

201	Implementation of hybrid pattern search–genetic algorithm into optimizing axial-flux permanent magnet coreless generator (AFPMG). Electrical Engineering, 2017, 99, 751-761.	1.2	13
202	Osteogenic priming potential of bovine hydroxyapatite sintered at different temperatures for tissue engineering applications. Materials Letters, 2017, 197, 83-86.	1.3	13
203	Improved ionic conductivity and efficiency of dye-sensitized solar cells with the incorporation of 1-methyl-3-propylimidazolium iodide. Ionics, 2020, 26, 3173-3183.	1.2	13
204	Augmentation of dye-sensitized solar cell photovoltaic conversion efficiency via incorporation of terpolymer Poly(vinyl butyral-co-vinyl alcohol-co-vinyl acetate) based gel polymer electrolytes. Polymer, 2021, 223, 123713.	1.8	13
205	Review on the Revolution of Polymer Electrolytes for Dye-Sensitized Solar Cells. Energy & Fuels, 2021, 35, 19320-19350.	2.5	13
206	Utilisation of corn starch in production of â€~green' polymer electrolytes. Materials Research Innovations, 2011, 15, s13-s8.	1.0	12
207	Effect of sintering temperature on structural properties of LiMnPO4 cathode materials obtained by sol–gel method. Journal of Sol-Gel Science and Technology, 2016, 80, 514-522.	1.1	12
208	Efficiency of supercapacitor using EC/DMC-based liquid electrolytes with methyl methacrylate (MMA) monomer. lonics, 2016, 22, 107-114.	1.2	12
209	Enhancing efficiency of dye sensitized solar cells based on poly(propylene) carbonate polymer gel electrolytes incorporating double salts. Ionics, 2020, 26, 493-502.	1.2	12
210	Co-regulative effects of chitosan-fennel seed extract system on the hormonal and biochemical factors involved in the polycystic ovarian syndrome. Materials Science and Engineering C, 2020, 117, 111351.	3.8	12
211	Influence of tetraglyme towards magnesium salt dissociation in solid polymer electrolyte for electric double layer capacitor. Journal of Polymer Research, 2020, 27, 1.	1.2	12
212	Rectify the performance of Green Building Rating Tool (GBRT) in sustainability: Evidence from ISO 21929-1. Journal of Cleaner Production, 2021, 278, 123378.	4.6	12
213	Effect of Sintering Profiles on the Properties and Ageing Resistance of Y-TZP Ceramic. International Journal of Automotive and Mechanical Engineering, 2011, 4, 405-413.	0.5	12
214	Sintering behaviour of slip-cast Al2O3 – Y-TZP composites. Journal of Materials Science, 2000, 35, 5509-5515.	1.7	11
215	Tailor-made fumed silica-based nano-composite polymer electrolytes consisting of BmImTFSI ionic liquid. Iranian Polymer Journal (English Edition), 2012, 21, 273-281.	1.3	11
216	Energy Efficient Wind Turbine System based on Fuzzy Control Approach. Procedia Engineering, 2013, 56, 637-642.	1.2	11

#	Article	IF	CITATIONS
217	Mechanochemical Synthesis of Magnesium Doped Hydroxyapatite: Powder Characterization. Applied Mechanics and Materials, 0, 372, 62-65.	0.2	11
218	The Effect of Iron Oxide on the Mechanical and Ageing Properties of Y-TZP Ceramic. Key Engineering Materials, 2016, 701, 225-229.	0.4	11
219	Breakdown field enhancement of Si-based MOS capacitor by post-deposition annealing of the reactive sputtered ZrOxNy gate oxide. Applied Physics A: Materials Science and Processing, 2016, 122, 1.	1.1	11
220	Solid terpolymer electrolyte based on poly(vinyl butyralâ€∢i>coâ€vinyl alcoholâ€ <i>co</i> â€vinyl acetate) incorporated with lithium salt and tetraglyme for EDLCs. Journal of Applied Polymer Science, 2018, 135, 45902.	1.3	11
221	Enhanced efficiency in dye-sensitized solar cell based on zinc oxide-modified poly(ethylene oxide) gel electrolyte. Ionics, 2018, 24, 1221-1226.	1.2	11
222	Effect of 1-Hexyl-3-Methylimidazolium Iodide Ionic Liquid on Ionic Conductivity and Energy Conversion Efficiency of Solid Polymer Electrolyte-Based Nano-Crystalline Dye-Sensitized Solar Cells. Journal of Nanoscience and Nanotechnology, 2020, 20, 2423-2429.	0.9	11
223	Zinc-substituted hydroxyapatite produced from calcium precursor derived from eggshells. Ceramics International, 2021, 47, 33010-33019.	2.3	11
224	THE EFFECT OF COLD ISOSTATIC PRESSING ON THE SINTERABILITY OF SYNTHESIZED HA. Biomedical Engineering - Applications, Basis and Communications, 2004, 16, 199-204.	0.3	10
225	Effect of bulge shape on wrinkling formation and strength of stainless steel thin sheet. Materials & Design, 2012, 42, 37-45.	5.1	10
226	Estimation of oxide scale growth and temperature increase of high (9–12%) chromium martensitic steels of superheater tubes. Engineering Failure Analysis, 2013, 35, 380-386.	1.8	10
227	Two dimensional elastic deformations of functionally graded coated plates with clamped edges. Composites Part B: Engineering, 2013, 45, 1010-1022.	5.9	10
228	Effect of Copper Oxide and Manganese Oxide on Properties and Low Temperature Degradation of Sintered Y-TZP Ceramic. Journal of Materials Engineering and Performance, 2014, 23, 4328-4335.	1.2	10
229	Water absorption properties of kenaf fibre–poly(vinyl alcohol) composites. Materials Research Innovations, 2014, 18, S6-144-S6-146.	1.0	10
230	Fatigue crack growth of a corner crack in a square prismatic bar under combined cyclic torsion–tension loading. International Journal of Fatigue, 2014, 64, 67-73.	2.8	10
231	Sinterability of Forsterite Prepared via Solidâ€5tate Reaction. International Journal of Applied Ceramic Technology, 2015, 12, 437-442.	1.1	10
232	Influences of sintering temperatures and crystallite sizes on electrochemical properties of LiNiPO4 as cathode materials via sol–gel route for lithium ion batteries. Journal of Sol-Gel Science and Technology, 2017, 83, 12-18.	1.1	10
233	Sintering behaviour of fluorapatite–silicate composites produced from natural fluorapatite and quartz. Ceramics International, 2021, 47, 16483-16490.	2.3	10
234	Effect of carbonate content on the in vitro bioactivity of carbonated hydroxyapatite. Ceramics International, 2022, 48, 18174-18179.	2.3	10

#	Article	IF	CITATIONS
235	Structural, morphological, thermal, and conductivity studies of magnesium ion conducting P(VdFâ€HFP)â€based solid polymer electrolytes with good prospects. Journal of Applied Polymer Science, 2010, 117, 2050-2058.	1.3	9
236	Prediction of Conductivity by Adaptive Neuro-Fuzzy Model. PLoS ONE, 2014, 9, e92241.	1.1	9
237	Synthesis and Properties of Biphasic Calcium Phosphate Prepared by Different Methods. Advanced Materials Research, 0, 970, 20-25.	0.3	9
238	Enhanced electrochemical properties of ZnO-coated LiMnPO4 cathode materials for lithium ion batteries. Ionics, 2016, 22, 1551-1556.	1.2	9
239	Effects of thermal oxidation duration on the structural and electrical properties of Nd2O3/Si system. Applied Physics A: Materials Science and Processing, 2017, 123, 1.	1.1	9
240	Electrical property enhancement of poly (vinyl alcohol-co-ethylene)–based gel polymer electrolyte incorporated with triglyme for electric double-layer capacitors (EDLCs). Ionics, 2021, 27, 361-373.	1.2	9
241	Linking the Development of Building Sustainability Assessment Tools with the Concept Evolution of Sustainable Buildings. Sustainability, 2021, 13, 12909.	1.6	9
242	Investigation of dibutyl phthalate as plasticizer on poly(methyl methacrylate)–lithium tetraborate based polymer electrolytes. Ionics, 2011, 17, 29-34.	1.2	8
243	Effect of Grain Size on Vickers Microhardness and Fracture Toughness in Calcium Phosphate Bioceramics. Applied Mechanics and Materials, 0, 83, 237-243.	0.2	8
244	The Governance of Sintering Regimes on the Properties and Ageing Resistance of Y-TZP Ceramic. Advanced Materials Research, 2012, 545, 81-87.	0.3	8
245	Sliding behavior of droplet on a hydrophobic surface with hydrophilic cavities: A simulation study. Physics of Fluids, 2018, 30, 122006.	1.6	8
246	Predicting the Primitive Form of Rhombohedral Silicon Carbide (9R-SiC): A Pathway toward Polytypic Heterojunctions. Crystal Growth and Design, 2018, 18, 7059-7064.	1.4	8
247	Effect of Air and Argon Sintering Atmospheres on Properties and Hydrothermal Aging Resistance of Y-TZP Ceramics. Journal of Materials Engineering and Performance, 2018, 27, 3574-3580.	1.2	8
248	Biological responses of MC3T3-E1 on calcium carbonate coatings fabricated by hydrothermal reaction on titanium. Biomedical Materials (Bristol), 2020, 15, 035004.	1.7	8
249	Biogenic integrated ZnO/Ag nanocomposite: Surface analysis and in vivo practices for the management of type 1 diabetes complications. Colloids and Surfaces B: Biointerfaces, 2020, 189, 110878.	2.5	8
250	Tetrahedral meshing for a slanted semi-elliptical surface crack at a solid cylinder. Engineering Fracture Mechanics, 2021, 241, 107400.	2.0	8
251	Effect of electrode substrate and poly(acrylamide) hydrogel electrolytes on the electrochemical performance of supercapacitors. Ionics, 2021, 27, 4507-4519.	1.2	8
252	Sintering Effects on the Densification of Nanocrystalline Hydroxyapatite. International Journal of Automotive and Mechanical Engineering, 2011, 3, 249-255.	0.5	8

#	Article	IF	CITATIONS
253	Densification of copper oxide doped alumina toughened zirconia by conventional sintering. Ceramics International, 2022, 48, 6287-6293.	2.3	8
254	Characterization of Forsterite Bioceramics. Advanced Materials Research, 0, 576, 195-198.	0.3	7
255	Effect of manganese oxide on the sinterability of 8 mol% yttria-stabilized zirconia. Materials Characterization, 2016, 120, 331-336.	1.9	7
256	Interfacial Reaction Analysis of Cu-Sn-Ni-P/Cu Joint Using Microwave Hybrid Heating. Key Engineering Materials, 0, 701, 148-153.	0.4	7
257	Formation of neodymium oxide by thermal oxidation of sputtered Nd thin film on Si substrate. Journal of Materials Science: Materials in Electronics, 2017, 28, 11994-12003.	1.1	7
258	Analysis of surface cracks in round bars using dual boundary element method. Engineering Analysis With Boundary Elements, 2018, 93, 112-123.	2.0	7
259	Influence of Magnesium Doping in Hydroxyapatite Ceramics. IFMBE Proceedings, 2008, , 326-329.	0.2	7
260	Effect of Copper Oxide on the Sintering of Alumina Ceramics. Advanced Materials Research, 0, 47-50, 801-804.	0.3	6
261	Development of Magnesium-Doped Biphasic Calcium Phosphatethrough Sol-Gel Method. IFMBE Proceedings, 2008, , 314-317.	0.2	6
262	Sodium-Doped Hydroxyapatite Nanopowder through Sol-Gel Method: Synthesis and Characterization. Materials Science Forum, 0, 694, 128-132.	0.3	6
263	Phase behaviour of manganeseâ€doped biphasic calcium phosphate ceramics synthesized via solâ€gel method. Asia-Pacific Journal of Chemical Engineering, 2011, 6, 823-831.	0.8	6
264	Numerical Simulation and Experimentation of Warm Metal Powder Compaction Process. Key Engineering Materials, 2011, 462-463, 704-709.	0.4	6
265	Sintering Behavior of Nanocrystalline Hydroxyapatite Produced by Wet Chemical Method. Current Nanoscience, 2011, 7, 845-849.	0.7	6
266	Concentration effect of BMIMTf on P(VdF-HFP)/MgTf-based solid polymer electrolyte system. Journal of Materials Research, 2012, 27, 1488-1496.	1.2	6
267	Notch root strain measurement of WE43-T6 magnesium alloy using electronic speckle pattern interferometry. Materials & Design, 2013, 51, 206-211.	5.1	6
268	Pre-implementation Study of Blended Learning in an Engineering Undergraduate Programme: Taylor's University Lakeside Campus. Procedia, Social and Behavioral Sciences, 2013, 103, 735-743.	0.5	6
269	Resistance Element Welding of Magnesium Alloy/austenitic Stainless Steel. IOP Conference Series: Materials Science and Engineering, 2017, 238, 012004.	0.3	6
270	Physicochemical and biological status of Aghlagan river, Iran: effects of seasonal changes and point source pollution. Environmental Science and Pollution Research, 2021, 28, 15339-15349.	2.7	6

#	Article	IF	CITATIONS
271	Chemo-physico-mechanical characteristics of high-strength alkali-activated mortar containing non-traditional supplementary cementitious materials. Journal of Building Engineering, 2021, 44, 103368.	1.6	6
272	Virtual Worlds: The Next Generation for Solving Engineering Problems. , 2008, , .		5
273	Synthesis of Strontium-Doped Hydroxyapatite Powder via Sol-Gel Method. Advanced Materials Research, 0, 47-50, 928-931.	0.3	5
274	Synthesis of High Fracture Toughness of Hydroxyapatite Bioceramics. Advanced Materials Research, 0, 264-265, 1849-1855.	0.3	5
275	Sintering of Hydroxyapatite Ceramic Produced by Wet Chemical Method. Advanced Materials Research, 0, 264-265, 1856-1861.	0.3	5
276	Fatigue growth of a surface crack in a V-shaped notched round bar under cyclic tension. Journal of Zhejiang University: Science A, 2014, 15, 873-882.	1.3	5
277	Amelioration of electrochemical and photovoltaic performances on P(VPâ€ <i>co</i> â€VAc) based gel polymer electrolyte by incorporating double salt for dyeâ€sensitized solar cells. Journal of Applied Polymer Science, 2016, 133, .	1.3	5
278	Effects of anodisation parameters on thin film properties: A review. Materials Science and Technology, 2017, 33, 699-711.	0.8	5
279	Investigation of the effect of anodization time and annealing temperature on the physical properties of ZrO <sub>2</sub> thin film on a Si substrate. Materials Research Express, 2017, 4, 086414.	0.8	5
280	Empirical solutions for stress intensity factors of a surface crack in a solid cylinder under pure torsion. Engineering Fracture Mechanics, 2018, 193, 122-136.	2.0	5
281	Development of a fuzzy-TOPSIS multi-criteria decision-making model for material selection with the integration of safety, health and environment risk assessment. Proceedings of the Institution of Mechanical Engineers, Part L: Journal of Materials: Design and Applications, 2021, 235, 1532-1550.	0.7	5
282	Current challenges and trends of interactive multimedia in enhancing engineering education. , 0, , .		4
283	Novel Chemical Conversion of Eggshell to Hydroxyapatite Powder. IFMBE Proceedings, 2008, , 333-336.	0.2	4
284	The Evaluation of Miscibility of Poly(vinyl Chloride) and Poly(ethylene Oxide) Blends by DSC, Refractive Index and XRD Analyses. International Polymer Processing, 2009, 24, 354-358.	0.3	4
285	Synthesis of Zinc Doped-Biphasic Calcium Phosphate Nanopowder via Sol-Gel Method. Key Engineering Materials, 2012, 531-532, 614-617.	0.4	4
286	Role of mechanical alloying parameters on powder distribution of Al/Cu alloy and Al/Cu composite. Materials Research Innovations, 2014, 18, S6-190-S6-195.	1.0	4
287	Scratch resistance enhancement of 3-glycidyloxypropyltrimethoxysilane coating incorporated with silver nanoparticles. Surface Engineering, 2014, 30, 177-182.	1.1	4
288	Sintering properties and thermal depletion of boron in zirconia–zirconium diboride conductive ceramic. Ceramics International, 2014, 40, 13313-13320.	2.3	4

#	Article	IF	CITATIONS
289	Study on the effects of milling time and sintering temperature on the sinterability of forsterite (Mg <sub>2</sub> SiO <sub>4</sub> ). Journal of the Ceramic Society of Japan, 2015, 123, 1032-1037.	0.5	4
290	Sintering and properties of magnesium orthosilicate ceramic. Ceramics International, 2015, 41, 13614-13623.	2.3	4
291	Comparative study on characteristics of laser welded-brazed AZ31/Ti-6Al-4V lap joints with and without coatings. International Journal of Advanced Manufacturing Technology, 2019, 101, 1023-1040.	1.5	4
292	Nonsurfactant Synthesis and Characterizations of Metal-Organic Framework MOF-5 Materials Using Fatty Alcohols. Science of Advanced Materials, 2014, 6, 1638-1644.	0.1	4
293	Phase Analysis and Densification of Steatite-based Ceramics. International Journal of Automotive and Mechanical Engineering, 2010, 1, 38-45.	0.5	4
294	Renewable and soft dynamic supercapacitors based on poly (acrylamide) hydrogel electrolytes and porous carbon electrodes. Polymer Bulletin, 2023, 80, 1285-1302.	1.7	4
295	Electrochemical performance of binder-free Ni(OH) <sub>2</sub> /RGO battery type electrode materials for supercapacitor. International Journal of Green Energy, 2023, 20, 725-733.	2.1	4
296	Effect of Slurry Preparation on Physical Properties of Porous Hydroxyapatite Prepared via Polymeric Sponge Method. Advanced Materials Research, 0, 47-50, 932-935.	0.3	3
297	Facile Preparation and Characterizations of Potential Low-Cost Nanostructured Materials for Energy Gas Storage. ECS Transactions, 2010, 28, 57-65.	0.3	3
298	Sintering and Densification Behavior of ZnO-Doped Y-TZP Ceramics. Applied Mechanics and Materials, 2011, 83, 197-203.	0.2	3
299	Effect of Nano Silica on the Sinterability of Hydroxyapatite Dense Bodies. Advanced Materials Research, 2011, 264-265, 1832-1838.	0.3	3
300	Porous Alumina from Protein Foaming-Consolidation Method Containing Hydrothermal Derived Hydroxyapatite Powder. Applied Mechanics and Materials, 0, 117-119, 782-785.	0.2	3
301	Pressureless Sintering of Electro-Conductive Zirconia Composites. Materials Science Forum, 2011, 694, 304-308.	0.3	3
302	Atypical behaviors of BMIMTf ionic liquid present in ionic conductivity, SEM, and TG/DTG analyses of P(VdF-HFP)/LiTf-based solid polymer electrolyte system. Journal of Materials Research, 2011, 26, 2945-2951.	1.2	3
303	Carbothermal nitridation process of mechanically milled silica sand using Taguchi's method. Ceramics International, 2013, 39, 6119-6130.	2.3	3
304	Oxygen Vacancy Comparisons for 3Y - TZP Sintered in Air and Argon Gas Atmosphere. Applied Mechanics and Materials, 2013, 372, 173-176.	0.2	3
305	Synthesis of Cu3.21Bi4.79S9 bismuth chalcogenide by mechanical alloying. Powder Technology, 2016, 294, 348-352.	2.1	3
306	A novel method of brazing Cu/Cuâ€7.0Niâ€9.3Snâ€6.3P/Cu using microwave hybrid heating. Materialwissenschaft Und Werkstofftechnik, 2017, 48, 299-305.	0.5	3

#	Article	IF	CITATIONS
307	Optimization of electrocoagulation process for the treatment of landfill leachate. IOP Conference Series: Materials Science and Engineering, 2017, 210, 012008.	0.3	3
308	Quasi-Solid Polymer Electrolyte Composed of poly(1-vinylpyrrolidone- <i>co</i> -vinyl acetate) Copolymer and the Influence of Its Composition on Electrochemical Properties and the Performances of Dye-Sensitized Solar Cells. Polymer-Plastics Technology and Engineering, 2018, 57, 98-107.	1.9	3
309	Rapid Nucleation of Reduced Graphene Oxide-Supported Palladium Electrocatalysts for Methanol Oxidation Reaction. Journal of Nanoscience and Nanotechnology, 2019, 19, 7236-7243.	0.9	3
310	Synthesis and properties of bioâ€wasteâ€based hydroxyapatite via hydrothermal process. Materialwissenschaft Und Werkstofftechnik, 2020, 51, 706-712.	0.5	3
311	The Effects of Sintering Additives on the Sintering of 3Y-TZP Ceramic. IOP Conference Series: Materials Science and Engineering, 2021, 1117, 012010.	0.3	3
312	Electrochemical studies of 1,2,3-Benzotriazole inhibitor for acrylic-based coating in different acidic media systems. Journal of Polymer Research, 2020, 27, 1.	1.2	3
313	Influence of calcination temperature in synthesizing eggshell-derived calcium phosphate. Materials Today: Proceedings, 2022, 48, 1915-1919.	0.9	3
314	Closed-Form Solutions of Stress Intensity Factors for Semi-elliptical Surface Cracks in a Cylindrical Bar Under Pure Tension. Acta Mechanica Solida Sinica, 2022, 35, 344-356.	1.0	3
315	PHASE STABILITY AND MICROSTRUCTURAL DEVELOPMENT OF Y-TZP–DOPED HYDROXYAPATITE. Biomedical Engineering - Applications, Basis and Communications, 2001, 13, 66-71.	0.3	2
316	Hydrocarbon templated sol-gel synthesis and characterizations of mesoporous silica xerogel. Studies in Surface Science and Catalysis, 2007, 165, 21-24.	1.5	2
317	Microemulsion Synthesis of Nanoparticle PZT Powder. AIP Conference Proceedings, 2011, , .	0.3	2
318	Dependence of the Fracture Toughness on the Sintering Time of Dense Hydroxyapatite Bioceramics. Materials Science Forum, 2011, 694, 391-395.	0.3	2
319	Mixed doped lithium nickel vanadate as cathode material by sol–gel and polymer precursor method. Materials Research Innovations, 2011, 15, s86-s91.	1.0	2
320	Fabrication of Porous Ceramic Scaffolds via Polymeric Sponge Method Using Sol-Gel Derived Strontium Doped Hydroxyapatite. Applied Mechanics and Materials, 0, 117-119, 829-832.	0.2	2
321	Intelligent air-cushion tracked vehicle performance investigation: neural-networks. International Journal of Heavy Vehicle Systems, 2012, 19, 407.	0.1	2
322	Characteristics of Sintered Bovine Hydroxyapatite. Applied Mechanics and Materials, 0, 372, 177-180.	0.2	2
323	Effect of sintering holding time on low-temperature degradation of yttria stabilised zirconia ceramics. Materials Research Innovations, 2014, 18, S6-408-S6-411.	1.0	2
324	Effect of microwave hybrid heating on the formation of intermetallic compound of Sn-Ag-Cu solder joints. , 2014, , .		2

#	Article	IF	CITATIONS
325	Fuzzy logic-based model for prediction of building wall humidity level. Indoor and Built Environment, 2014, 23, 565-573.	1.5	2
326	Effect of MgO addition on the sinterability, mechanical properties and biological cell activities of sintered silicon-substituted hydroxyapatite. Journal of the Australian Ceramic Society, 2021, 57, 857.	1.1	2
327	Influence of Magnesium Doping in Hydroxyapatite Bioceramics Sintered by Short Holding Time. IFMBE Proceedings, 2011, , 80-83.	0.2	2
328	Densification and Mechanical Properties of Alumina Ceramics via Two-Step Sintering With Different Holding Times. International Journal of Engineering Materials and Manufacture, 2021, 6, 299-304.	0.2	2
329	Performance investigation of electrocoagulation and Electro-Fenton processes for high strength landfill leachate: operational parameters and kinetics. Chemical Papers, 2022, 76, 2991-3003.	1.0	2
330	SYNTHESIS AND REDOX BEHAVIOR OF OXYGEN DEFICIENT BRANNERITE <font>LiVWO</font> <sub>6-δ</sub> FOR LITHIUM BATTERIES. , 2002, , .		1
331	Development of interactive multimedia in teaching engineering materials. , 0, , .		1
332	Bioactive porous ceramics via polymeric sponge method: the effect of preparation conditions on physical properties. , 2007, , .		1
333	Investigation of wall-slip behavior in lead-free solder pastes and isotropic conductive adhesives. , 2009, , .		1
334	Sintering behaviour of forsterite bioceramics. , 2011, , .		1
335	Effects of Powder Synthesis Method on the Sinterability of Hydroxyapatite. Advanced Materials Research, 2011, 264-265, 1538-1544.	0.3	1
336	Role of physical and mechanical properties of stainless steels in expected thermal fatigue life of plenum barrier plate of a gas turbine frame. Engineering Failure Analysis, 2011, 18, 2336-2342.	1.8	1
337	Effects of Bismuth Oxide on the Properties of Calcium Phosphate Bioceramics. Advanced Materials Research, 0, 264-265, 1839-1848.	0.3	1
338	PALM OIL BASED FATTY ALCOHOLS TEMPLATED MESOPOROUS SILICA AND SILICA SPHERES. International Journal of Nanoscience, 2011, 10, 1275-1281.	0.4	1
339	Mechanical and Electrical Properties of Y-TZP/ZrB <sub>2</sub> Composite. Advanced Materials Research, 0, 576, 228-231.	0.3	1
340	Effect of Ultrasonication on Synthesis of Forsterite Ceramics. Advanced Materials Research, 0, 576, 252-255.	0.3	1
341	Sintered Properties of Y-TZP/ZrB <sub>2</sub> Ceramics. Applied Mechanics and Materials, 2013, 372, 169-172.	0.2	1
342	Densification Behavior of Nano Y-TZP Ceramics. Applied Mechanics and Materials, 2013, 372, 165-168.	0.2	1

#	Article	IF	CITATIONS
343	The effect of sintering ramp rate on the sinterability of forsterite ceramics. Materials Research Innovations, 2014, 18, S6-61-S6-64.	1.0	1
344	Implementation of a Voice-ControlSystem for Issuing Commands in a Virtual Manufacturing Simulation Process. Advanced Materials Research, 0, 980, 165-171.	0.3	1
345	Development of Sn–Cu–Sb alloys for making lead- and bismuth-free pewter. International Journal of Materials Research, 2014, 105, 183-187.	0.1	1
346	Sintering properties of zirconia-based ceramic composite. Materials Research Innovations, 2014, 18, S6-105-S6-108.	1.0	1
347	Thermal treatment and properties of bovine hydroxyapatite. Materials Research Innovations, 2014, 18, S6-117-S6-120.	1.0	1
348	Low-temperature degradation and defect relationship in yttria-tetragonal zirconia polycrystal ceramic. Materials Research Innovations, 2014, 18, S6-131-S6-134.	1.0	1
349	Magnesium Doped Hydroxyapatite through Mechanochemical Synthesis. Advanced Materials Research, 0, 1087, 329-333.	0.3	1
350	The effects of zinc oxide on the sinterability of hydroxyapatite. , 2016, , .		1
351	Effect of ZnO addition on the purity and densification of forsterite ceramic. IOP Conference Series: Materials Science and Engineering, 2017, 206, 012051.	0.3	1
352	Nucleation and growth controlled reduced graphene oxide–supported palladium electrocatalysts for methanol oxidation reaction. Nanomaterials and Nanotechnology, 2019, 9, 184798041982717.	1.2	1
353	Influence of sintering profile on the mechanical properties of manganese oxide doped 3Y-TZP. IOP Conference Series: Earth and Environmental Science, 2020, 463, 012094.	0.2	1
354	Sintering Behavior of Hydroxyapatite Ceramics Prepared by Different Routes. Ceramic Engineering and Science Proceedings, 0, , 127-137.	0.1	1
355	Numerical Investigation of the Behaviour of Thin-Walled Metal Tubes Under Axial Impact. Lecture Notes in Mechanical Engineering, 2019, , 55-64.	0.3	1
356	Influence of powder morphology and sintering temperature on the properties of hydroxyapatite. International Journal of Automotive and Mechanical Engineering, 2015, 12, 3089-3096.	0.5	1
357	Effects of Selection of Inlet Perturbations, Multiphase and Turbulence Equations on Slug Flow Characteristics Using Altair® AcuSolve™. Processes, 2021, 9, 2152.	1.3	1
358	Characterization and Sintering Properties of Hydroxyapatite Bioceramics Synthesized From Clamshell Biowaste. IIUM Engineering Journal, 2022, 23, 228-236.	0.5	1
359	DYNAMIC ANALYSIS OF THE HUMAN KNEE. Biomedical Engineering - Applications, Basis and Communications, 2002, 14, 122-126.	0.3	0
360	EFFECT OF COPPER OXIDE ADDITIONS ON THE GRAIN BOUNDARY RESISTIVITY IN YTTRIA–TETRAGONAL ZIRCONIA. , 2002, , .		0

#	Article	IF	CITATIONS
361	Sinterability Of Hydroxyapatite Compacts Prepared By Cold Isostatic Pressing For Clinical Applications. IFMBE Proceedings, 2007, , 137-140.	0.2	0
362	Facile Synthesis and Characterizations of MOF-5 Coordination Polymer with Various Metal Linker Ratios for Ammonia Gas Storage. , 2011, , .		0
363	Synthesis and Structural Consideration of Metal-Organic Framework (MOF) Coordination Polymer with Various Metal Linker Ratios. Key Engineering Materials, 0, 462-463, 1103-1108.	0.4	0
364	The Effect of Ball Milling Hours in the Synthesizing Nano-Crystalline Forsterite via Solid-State Reaction. IFMBE Proceedings, 2011, , 102-104.	0.2	0
365	The Influence of Manganese Oxide on the Sintering Behavior of Yttria Tetragonal Zirconia. , 2011, , .		0
366	Mechanochemical Synthesis of Hydroxyapatite Bioceramics through Two Different Milling Media. Key Engineering Materials, 2012, 531-532, 254-257.	0.4	0
367	Protein Foaming-Consolidation Method for Fabrication of High Performance Porous Bioceramics. Advanced Materials Research, 0, 622-623, 1759-1763.	0.3	0
368	Effects of Ramp Rates with Short Holding Time on the Sinterability of Hydroxyapatite. Advanced Materials Research, 0, 545, 229-234.	0.3	0
369	Facile Processing of γ-Alumina for Potential Energy Storage. Advanced Materials Research, 0, 576, 402-405.	0.3	0
370	Densification Behavior of Steatite by Two Stage Sintering. Advanced Materials Research, 0, 488-489, 194-201.	0.3	0
371	Characterization of Forsterite Synthesized by Solid-State Reaction with Ball Milling Method. Applied Mechanics and Materials, 0, 372, 416-419.	0.2	0
372	Sintering studies of synthesised manganese-oxide-doped calcium phosphate via wet chemical precipitation method. Materials Research Innovations, 2014, 18, S6-147-S6-150.	1.0	0
373	Effect of Attritor Milling on Synthesis and Sintering of Forsterite Ceramics. International Journal of Applied Ceramic Technology, 2016, 13, 726-735.	1.1	0
374	Effects of anodization duration on the properties of sputtered samarium thin films on silicon substrate. Journal of Materials Science: Materials in Electronics, 2016, 27, 4988-4995.	1.1	0
375	Evaluation of Thermoelectric Properties of Cu <sub>3.21</sub> Bi <sub>4.79</sub> S <sub>9</sub> Bismuth Chalcogenide. Key Engineering Materials, 0, 701, 220-224.	0.4	0
376	Effects of Resin Binder on Characteristics of Sintered Aluminum–Copper Nanopaste as High-Temperature Die-Attach Material. IEEE Transactions on Components, Packaging and Manufacturing Technology, 2019, 9, 2104-2110.	1.4	0
377	Investigation of Energy Absorption Behaviour of Square Aluminium Tubes with Cutouts under Axial Compression. Materials Science Forum, 0, 969, 181-186.	0.3	0
378	Sinterability of Calcium Phosphate Through Rapid Sintering. Journal of Physics: Conference Series, 2021, 1892, 012038.	0.3	0

#	Article	IF	CITATIONS
379	Surface yttria content and hydrothermal ageing behaviour of two step sintered 3Y-TZP ceramics. Journal of the National Science Foundation of Sri Lanka, 2021, 49, 219.	0.1	0
380	DENSIFICATION BEHAVIOUR OF CuO-DOPED Al2O3 CERAMICS. , 2001, , .		0
381	CAL Student Coaching Environment and Virtual Reality in Mechanical Engineering. International Journal of Information and Communication Technology Education, 2006, 2, 12-27.	0.8	0
382	Sintering Behaviour of TiO2-Doped Alumina for Biomedical Application. IFMBE Proceedings, 2008, , 351-353.	0.2	0
383	Technology Assisted Problem Packages For Engineering. Advances in Information and Communication Technology Education Series, 2008, , 73-87.	0.1	0
384	Sintering and Mechanical Properties of MgO-Doped HA Bioceramic. Advanced Science Letters, 2012, 14, 278-280.	0.2	0
385	Densification and Mechanical Properties of Y-TZP/25 wt. % ZrB2 Composite. Jurnal Teknologi (Sciences) Tj ETQq1	10,7843 0,3	14 rgBT /Ov
386	Technology Assisted Problem Packages For Engineering. , 0, , .		0
387	Low-temperature degradation behaviour of microwave sintered CuO-doped Y-TZP ceramics. Materials Today: Proceedings, 2022, , .	0.9	0